# Potential of zero charge and surface charging relation of metal-solution interphases from a constant-potential jellium-Poisson-Boltzmann model

Jun Huang [1,*] Peng Li,[2] and Shengli Chen[2,†]

[1]*Hunan Provincial Key Laboratory of Chemical Power Sources, College of Chemistry and Chemical Engineering, Central South University, Changsha 410083, China*

[2]*Hubei Key Laboratory of Electrochemical Power Sources, Key Laboratory of Analytical Chemistry for Biology and Medicine (Ministry of Education), Department of Chemistry, Wuhan University, Wuhan 430072, China*

(Received 20 June 2019; revised manuscript received 22 February 2020; accepted 26 February 2020; published 23 March 2020)

The potential of zero charge (pzc), a fundamental concept in interfacial electrochemistry, is revisited using a jellium-Poisson-Boltzmann model. Under constant-potential description of the metal-solution interphase, this model is able to calculate the surface charging relation (surface free charge density as a function of the electrode potential) and then to determine the pzc therefrom. The potential corresponding to the minimum of differential double-layer capacitance curve is shown to be lower than the pzc determined from surface charging relation, which is caused by free metal electrons entering the solution phase. The model further reveals that the pzc decreases when the vacuum gap between the solution phase and the metal surface, $d$, becomes narrower. This is consistent with the common observation that the pzc of metal-solution interphase is lower than that calculated from the work function of metal-vacuum interphase (the latter corresponds to $d = \infty$). Multifaceted roles played by the solvent, including electrostatic screening, polaron effect, and orthogonalizational repulsion, are analyzed. Also discussed are the effects of specific adsorption of ions and potential-dependent $d$ on the surface charging relation.

DOI: 10.1103/PhysRevB.101.125422

## I. INTRODUCTION

The potential of zero charge (pzc), also termed as point of zero charge, is defined as the potential, usually referenced to the standard hydrogen electrode (SHE), at which there is no free-electrode charge, defined as the net charge of free metal electrons and metal ions, to be mathematically expressed in Eq. (12) [1]. For a metal-solution interphase, pzc plays a role similar to that of work function for a metal-vacuum interphase; it is a basic property containing substantial microscopic information of the metal, the solution, and the interphase with complex interactions in between [2]. When the electrode potential deviates from the pzc, the metal-solution interphase becomes electrified, attracting counterions into the interphase and forming a diffuse layer where potential and concentration vary greatly and electrochemical reactions, if any, occur. As a result, the pzc is of fundamental significance in understanding electrode kinetics [3–6].

Coined by Frumkin in 1928 [7], the pzc attracts unabated interests in both experimental and theoretical electrochemistry [2,8–11]. As regards simple metals in a nonspecifically adsorbing electrolyte, such as mercury in NaF solutions, the pzc can be derived from experimental differential double-layer capacitance curves using the Gouy-Chapman ansatz [1]. When specific adsorption and/or chemisorption comes into play, new complexities emerge, necessitating the distinction between the potential of zero free charge (pzfc) and the potential of zero total charge (pztc) [9,12,13]. To put it simply, the pzfc considers exclusively the free electrode charge, which is tuned by adding or removing free metal electrons and which is compensated by counterions in solution, while the pztc extends to all electrons entering or exiting from the electrode, including those hopping into/from the electron orbitals of particles (ions or molecules) in solution. The pztc, corresponding to the total current density measured, can be experimentally determined, for example, from voltammetry [13,14]. However, it is difficult to do the same for the pzfc, corresponding to the pure double-layer charging current density, because there is no reliable way to separate double-layer charging current density from total current density. As regards the impedance approach, the overlap between differential double-layer capacitance and pseudocapacitance of adsorption makes it difficult, if not impossible, to determine pzfc from differential double-layer capacitance curves [15]. Several remedies have been developed [11–13]. The CO displacement method measures total surface charge at Pt electrodes, from which the pzfc can be estimated by a linear extrapolation [11–14,16]. Apart from errors introduced in the linear extrapolation, the CO displacement method is inapplicable at high potentials (say $>0.5\ V_{RHE}$ where RHE refers to the reversible hydrogen electrode), due to CO oxidation. In its stead, the laser-induced temperature-jump method circumvents the extrapolation of total electrode charge curve and directly reflects the pzfc [12,17]. Recently, $N_2O$ and peroxodisulfate reduction reaction

*jhuangelectrochem@qq.com
†slchen@whu.edu.cn

 

of which the reactivity is sensitive to free electrode charge are developed to probe the pzfc [12,14,18,19]. The Alicante group led by Feliu is the major propellant of this research field [12,13,19].

Concomitant with continual activities from the experimental side are ongoing attempts of predicting the pzfc using first-principles calculations. In this vein, two key issues are encountered: description of the solvent environment, and the potential reference. As regards the former issue, Jinnouchi and Anderson employed a modified Poisson-Boltzmann to treat the solvent in an implicit manner [20], while Tripkovic *et al.* introduced several water layers explicitly into the simulation system [21], and, as a step further, Sakong *et al.* performed large-scale *ab initio* molecular-dynamics simulations which better simulate the liquid water [22]. As regards the latter issue, an experimental SHE scale is commonly used to convert the calculated work function into the pzc by a simple subtraction. Recently, Le *et al.* removed the need for an experimental SHE [23], and adopted a computational SHE method which was developed earlier by Cheng and Sprik [24]. Despite diversity in the computational methods, these computational works unravel that the work function and pzc of the metal covered by a water film are lowered due to two effects. On one hand, interfacial water molecules reorient and/or polarize, leading to a net dipole moment at the surface. On the other hand, free metal electrons redistribute upon addition of surface water. However, which effect dominates is a question open to dispute still [22,23].

Notwithstanding substantial progresses discussed above, understanding of the pzc is incomplete yet. Firstly, it is unclear how electrostatic interactions in the double layer influence the pzc, because most first-principles calculations to date are conducted in an ion-free environment under constant charge condition [25,26]. There are, indeed, several constant-potential schemes combining density-functional theory (DFT) and modified Poisson-Boltzmann theory [20,27,28]. However, emphasis has been put on calculating the pzc of different metals, while the influence of the solution side on the pzc is marginally discussed. Secondly, it is known that specific adsorption and chemisorption bring about dramatic influence on the surface charging relation of metal-solution interphases [9,18,29,30]. Nevertheless, existing theories rarely consider these factors. Last but not least, first-principles calculations are usually computationally expensive and case specific. There is a clear need for a simple and general theoretical description of metal-solution interphases including essential electronic and double-layer effects. In tackling these challenges, the continuum approach, able to describe the double layer under constant potential and to incorporate various short-range interactions between ions and metal electron in a phenomenological way, may complement quantum-mechanical approaches.

Herein, a continuum model, in which metal electronic effects are described by a jellium model and the solution side by a modified Poisson-Boltzmann model, is developed for conceptual understanding of the pzc. The model features a constant-potential description of the metal-solution interphase with a position-dependent dielectric constant, rendering calculation of the surface charging relation and then the determination of the pzc. Armed with this model, we dissect multifaceted effects of solvent on the pzc, scrutinize the definition of pzc, reexamine the correspondence between the pzc and the Gouy-Chapman minimum of the differential double-layer capacitance curve, and explore the effects of specific adsorption on the pzc. Albeit being unable to accurately describe a specific metal-solution interphase, this simple model contains essential parameters important to the pzc and identifies key problems for future first-principles investigations.

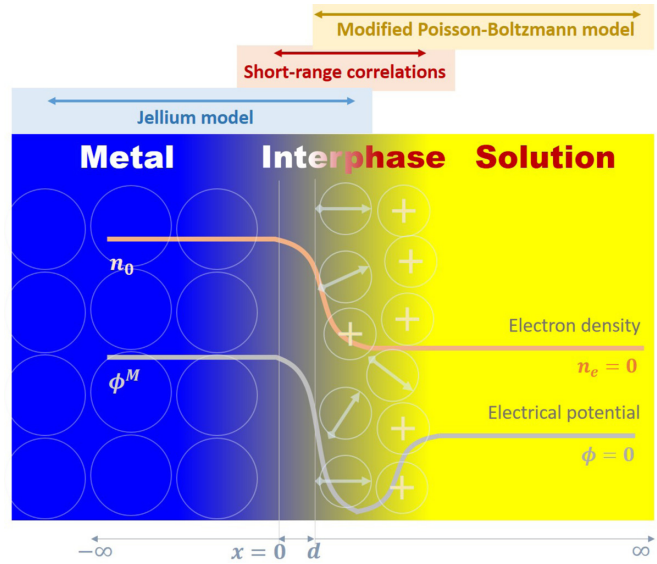


FIG. 1. Model schematic. The model describes the metal side by the jellium model, and the solution side by a modified Poisson-Boltzmann model. Short-range correlations between metal electrons and solvents as well as ions are included. Given the free-electron density in metal bulk, $n_0$, and the electrical potential in metal bulk, $\phi^{\mathrm{M}}$, the model gives out continuous distributions of the free-electron density and the electric potential from the metal bulk to the solution bulk.

## II. THE MODEL

The model consists of a "free-electron-like" metal and a monovalent symmetric electrolyte solution in a one-dimensional $x$ coordinate, as schematically shown in Fig. 1. The jellium edge is denoted as $x = 0$, the metal bulk as $x = -\infty$, and the solution bulk as $x = \infty$. The closest plane that solution species can approach the metal surface is denoted $x = d$. The electrical potential in the solution bulk is used as the potential reference.

The overarching task of calculating the pzc is transformed to the task of calculating the distribution of free metal electron density, $n_{\mathrm{e}}$, spanning from the metal bulk to the solution bulk as a function of the electrode potential and solution properties. We start with writing the free-energy density functional of the

metal-solution interphase,

$$f = \xi n_{\mathrm{ref}}\left(c_{\mathrm{k}} n_{\mathrm{e}}^{\frac{5}{3}} + \frac{c_{\mathrm{e}}}{\epsilon_{\mathrm{opt}}} n_{\mathrm{e}}^{\frac{4}{3}} + \frac{c_{\mathrm{c}}}{\epsilon_{\mathrm{opt}}} \frac{n_{\mathrm{e}}^{\frac{4}{3}}}{0.079 + \epsilon_{\mathrm{opt}} n_{\mathrm{e}}^{\frac{1}{3}}} + c_{\mathrm{g}} \frac{\left(\overset{\mathrm{a.u.}}{\nabla} n_{\mathrm{e}}\right)^2}{n_{\mathrm{e}}}\right)$$
$$+ \mathrm{e}_0 \phi n_{\mathrm{ref}}(n_0\theta(-x) - n_{\mathrm{e}} + (n_{\mathrm{c}} - n_{\mathrm{a}})\theta(x-d)) - \frac{\epsilon_0}{2}(1 + (\epsilon_{\mathrm{opt}} - 1)\theta(x-d))E^2$$
$$- k_{\mathrm{B}} T n_{\mathrm{ref}}\theta(x-d)\left(n_{\mathrm{s}} \ln\left(\frac{\sinh(pE\beta)}{pE\beta}\right) - \ln\frac{n_l!}{n_c! n_a! (n_l - n_a - n_c)!}\right) + \frac{n_{\mathrm{e}}}{n_0} n_{\mathrm{ref}}\theta(x-d)(n_s W_s + n_a W_a + n_c W_c). \quad (1)$$

The first line in Eq. (1) represents the metal electronic energy density using the jellium model, which was based on the density-functional formulism of Kohn *et al.* [31,32] that has been widely used in the theory of metal surface by Lang and Kohn [33,34] and introduced to the theory of double layer by Badiali *et al.* [35,36] and Schmickler [37] in 1980s. The jellium model treats the metal ionic charge as a positive background which ends at the jellium edge ($x = 0$), and free electrons as an inhomogeneous electron gas. The first three terms correspond to kinetic, exchange, and correlation energy densities of a homogeneous electron gas of density $n_{\mathrm{e}}$, respectively. Inhomogeneity effects are represented by the fourth term. The constants, $c_{\mathrm{k}} = 2.87$, $c_{\mathrm{e}} = -0.74$, $c_{\mathrm{c}} = -0.056$, and $c_{\mathrm{g}} = 0.014$, are respective interaction coefficients [38]. According to Kornyshev *et al.*, exchange-correlation interactions are screened by the fast part of the dielectric polarization, characterized by the optical dielectric constant $\epsilon_{\mathrm{opt}}$ [39,40]. Note that the electronic dielectric constant is given by $\epsilon_0(1 + (\epsilon_{\mathrm{opt}} - 1)\theta(x-d))$, which is reduced back to $\epsilon_0$ when $x < d$. $\xi = 27.2\,\mathrm{eV}$ is the atomic energy, a coefficient transforming from atomic units (a.u.) to SI units.

The second line describes the electrostatic energy density [41], where $e_0$ is the elementary charge, $\epsilon_o$ the dielectric constant of vacuum, $\phi$ the potential, $E$ the electrical field, $n_{\mathrm{ref}} = (a_0)^{-3}$ the reference number density, $a_0$ the Bohr radius, $n_0$ normalized (with respect to $n_{\mathrm{ref}}$, hereinafter) number density of metal ionic charge, $n_{\mathrm{c}}$ and $n_{\mathrm{a}}$ normalized number densities of cations and anions, respectively. $\theta(x)$ is the Heaviside function. $d$ denotes the distance between the jellium edge and the closest plane that solvent and ions can approach the metal surface. As for a hydrated ion, $d$ is the closest distance from the jellium edge to the hydration sphere.

The first term in the third line describes the field-dependent orientation of solvent molecules, where $n_{\mathrm{s}}$ is the normalized number density of solvent, $p$ the dipole moment of solvent, $\beta = 1/k_B T$ with $k_B$ being the Boltzmann constant, and $T$ the temperature. The logarithmic term for the free energy of solvent was developed by Booth [42] and widely used in the double-layer theory to describe dielectric saturation in the interfacial region [43]. The second term in the third line corresponds to the configuration entropy, calculated using a lattice-gas approach [44,45], of cations and anions in the solution side. $n_l$ denotes the normalized number density of lattice sites.

The fourth line describes the short-range correlations between free metal electrons and solvents as well as ions [46]. $W_i$ (unit: eV) characterizes the strength of short-range correlations between free metal electrons and species $i$ in the solution ($i = s$ for solvent, $i = a$ for anions, and $i = c$ for cations). The Heaviside function $\theta(x-d)$ implies that these short-range correlations act on free metal electrons stretching into the solution phase only. Herein, $n_e$ is normalized with respect to $n_0$ such that $W_i$ corresponds to the interaction with one metal electron.

Through the variational procedure, the free-energy density functional $f$ in Eq. (1) is submitted to two Euler-Lagrange equations in terms of $\phi$ and $n_{\mathrm{e}}$, respectively,

$$\frac{\partial f}{\partial \phi} - \frac{\partial}{\partial x}\left(\frac{\partial f}{\partial E}\right) = 0, \quad (2)$$

$$\frac{\partial f}{\partial n_{\mathrm{e}}} - \frac{\partial}{\partial x}\left(\frac{\partial f}{\partial(\nabla n_{\mathrm{e}})}\right) = 0. \quad (3)$$

Substituting Eq. (1) into Eq. (2) leads to a modified Poisson-Boltzmann (PB) equation considering dielectric saturation,

$$-\frac{\partial}{\partial X}\left(\epsilon_s \frac{\partial U}{\partial X}\right) = n_0\theta(-X) - n_{\mathrm{e}} + (n_{\mathrm{c}} - n_{\mathrm{a}})\theta(X - D), \quad (4)$$

where $X = x/\lambda$ is the dimensionless coordinate with $\lambda = (\epsilon_0 k_{\mathrm{B}} T / e_0^2 n_{\mathrm{ref}})^{-0.5}$ being the reference length sharing the same form of the Debye length, $D = d/\lambda$ is the dimensionless closest distance, $U = e_0\phi/k_{\mathrm{B}}T$ is the dimensionless potential, and $\epsilon_s$ is the dielectric constant, given by

$$\epsilon_s = 1 + \theta(X - D)\left((\epsilon_{\mathrm{opt}} - 1) + P n_{\mathrm{s}}\left(\frac{\partial U}{\partial X}\right)^{-1} L\left(P\frac{\partial U}{\partial X}\right)\right), \quad (5)$$

with $P = p/e_0\lambda$ being the dimensionless dipole moment of solvent, $L(x) = \coth(x) - 1/x$ is the Langevin function. Compared with the conventional PB equation, the modified PB equation in Eq. (4) has two distinct features. Firstly, it uses a potential-dependent dielectric constant given in Eq. (5) considering the field-dependent reorientation of solvent. Secondly, it extends to the metal phase involving metal ions and free electrons, in addition to cations and anions in solution.

In Eq. (4), $n_{\mathrm{c}}$ and $n_{\mathrm{a}}$ are determined by using the equilibrium condition that electrochemical potentials of cations and anions in the interfacial region should be equal to their values in the solution bulk, leading to the following identities:

$$\frac{\partial f}{\partial n_{\mathrm{c}}} = \left(\frac{\partial f}{\partial n_{\mathrm{c}}}\right)_{\mathrm{bulk}}, \quad (6)$$

$$\frac{\partial f}{\partial n_{\mathrm{a}}} = \left(\frac{\partial f}{\partial n_{\mathrm{a}}}\right)_{\mathrm{bulk}}. \quad (7)$$

Substituting Eq. (1) into Eq. (6) and (7) obtains

$$n_{\rm c} = n_{\rm c}^0 \frac{\exp(-U - n_e W_c)}{1 - \chi + \frac{\chi}{2}(\exp(-U - n_e W_c) + \exp(U - n_e W_a))}, \tag{8}$$

$$n_{\rm a} = n_{\rm a}^0 \frac{\exp(U - n_e W_a)}{1 - \chi + \frac{\chi}{2}(\exp(-U - n_e W_c) + \exp(U - n_e W_a))}, \tag{9}$$

where $n_{\rm c}^0$ and $n_{\rm a}^0$ are normalized number densities of cations and anions in the solution bulk, respectively, which are equal to each other for the current case; $\chi = (n_{\rm c}^0 + n_a^0)/n_l$ represents the occupancy of the lattice sites by ions in the solution. The modified Boltzmann relations in Eqs. (8) and (9) are reduced back to the conventional ones for the limiting case of $\chi = 0$ and $W_i = 0$.

Substituting Eq. (1) into Eq. (3) leads to a differential equation describing the distribution of free metal electrons,

$$\frac{\partial}{\partial X}\left(\frac{\partial n_{\rm e}}{\partial X}\right) = \frac{1}{2n_{\rm e}}\left(\frac{\partial n_{\rm e}}{\partial X}\right)^2 + \frac{\lambda^2}{2c_{\rm g}a_0}\Bigg(n_{\rm e}(\Upsilon(n_{\rm e}) - \Upsilon(n_0)), - \varsigma n_{\rm e}(U - U^M) + \frac{\varsigma n_{\rm e}\theta(X - D)}{k_{\rm B}T n_0}\sum_{i=s,a,c} n_i W_i\Bigg), \tag{10}$$

where $\varsigma = k_{\rm B}T/\xi$, $U^M$ is the dimensionless electrical potential applied onto the metal referenced to the potential in solution bulk, $\Upsilon(x)$ is a function derived from the jellium model, expressed as

$$\Upsilon(x) = \frac{5}{3}c_{\rm k}x^{2/3} + \frac{4}{3}\frac{c_{\rm e}}{\epsilon_{\rm opt}}x^{1/3} + \frac{c_{\rm c}}{\epsilon_{\rm opt}}\frac{\epsilon_{\rm opt}x^{2/3} + 0.105x^{1/3}}{(0.079 + \epsilon_{\rm opt}n_{\rm e}^{1/3})^2}. \tag{11}$$

Note in passing that the electron density profile was approximated by trial functions in vast majority of studies employing a "statistical" version of density-functional approach as a viable alternative (especially for *sp* metals) to more complicated quantum-mechanical density-functional calculations. In application to the models containing sharp variation of the dielectric and charge distribution profiles (as in our current model), it was reported that the results might be strongly dependent on the choice of trial functions. [46,47] This emphasizes the importance of finding electron density profiles by solving Eq. (10) directly, and thus removing the uncertainty introduced by trial functions.

Equations (4) and (10) are closed with following boundary conditions: in the metal bulk, $X = -\infty$, we have $U = U^M$ and $n_{\rm e} = n_0$, and in the solution bulk, $X = \infty$, we have $U = 0$ and $n_{\rm e} = 0$. Note that we have used the electrical potential in the solution bulk as the potential reference. Given the solution properties ($n_{\rm c}^0$, $n_l$, and $p$), the metal property ($n_0$), and the microstructure of the interphase ($d$), the metal-electrolyte interphase is exclusively controlled by the electrical potential ($U^M$).

The characteristics of the metal enter into this formulism only through $n_0$ which ranges between $1.33 \times 10^{-3}$ to $8.42 \times 10^{-2}$ for the metals "amenable to analysis using the free-electron model" [38] considered herein. As this model does not intend to mimic a specific metal, we designate $\rm n_0 = 10^{-2}$ for the base case. It is found that the choice of $n_0$ does not change the trends and conclusion obtained from this model. As regards the solution side, a 0.1-M monovalent symmetric electrolyte with water as the solvent is used for the base case. Therefore, we have $n_{\rm c}^0 = n_a^0 = 100\ {\rm N_A}$, with $N_{\rm A}$ being Avogadro constant, $n_l = 3.34 \times 10^{28}\ {\rm m}^{-3}$, and $p = 1.32 \times 10^{-29}$ C m such that the relative dielectric constant of the bulk water is 78.5. Note that this model neglects the size asymmetry between cations, anions, and solvent, and takes the solvent size as the lattice size. The closest distance, $d$, is a key interfacial property dictating the pzc; we take $d = 1$ Å as the base value and will discuss the $d$ effect at greater length later. We use $\epsilon_{\rm opt} = 1.8$ according to Kornyshev *et al.* [39] For the base case, we use $W_{\rm s} = 5$ eV for the orthogonalizational repulsion between metal electrons and solvents, and neglect specific adsorption of cations and anions, namely, $W_{\rm a} = W_{\rm c} = 0$ eV.

## III. RESULTS AND DISCUSSION

### A. Constant-potential description for double layer

Given parameters of the metal and solution, the model is solved at each constant potential, rendering the total number of free electrons in the system a potential-dependent variable. A constant-potential description of the metal-electrolyte interphase distinguishes our approach from the majority of previous double-layer models accounting for the effects of metal electrons by imposing fixed surface charge density condition (see Refs. [48,49] for review). In addition, it has been clearly demonstrated in Ref. [50,51] that the condition of fixed surface charge density is in general not equivalent to the condition of constant electrode charge because the former additionally requires that the charge is uniformly distributed in the plane of electrode. This requirement is not always satisfied in equilibrium. In a broader view, the differences between constant-potential and constant-charge descriptions have been discussed by Feldman *et al.* in 1986 [52]. It has been shown that a constant-charge description may result in negative double-layer capacitance, signifying instabilities and phase transitions of metal-solution interphases under constant-potential description [51–54]. Interested readers are referred to profound discussion in a review article written by Partenskii *et al.* [50] Several constant-potential computational schemes have been developed for electrochemical systems [21,27,28,55], such as the recent grand-canonical density-functional theory approach developed by Melander *et al.* [28]

Figure 2 shows model results for the base case with an electrode potential of $U^{\rm M} = 30$. Figure 2(a) portrays how $U$ distributes from the metal to the solution. Figure 2(b) shows that free metal electrons extend beyond the jellium edge and into the solution phase, a quantum-mechanical effect termed electron spillover in the literature [34]. A steep potential drop occurs at the jellium edge, which is caused by electron spillover. Leaving from the metal surface to the solution phase, $U$ increases towards positive values and approaches zero in the solution bulk, implying that the metal-solution

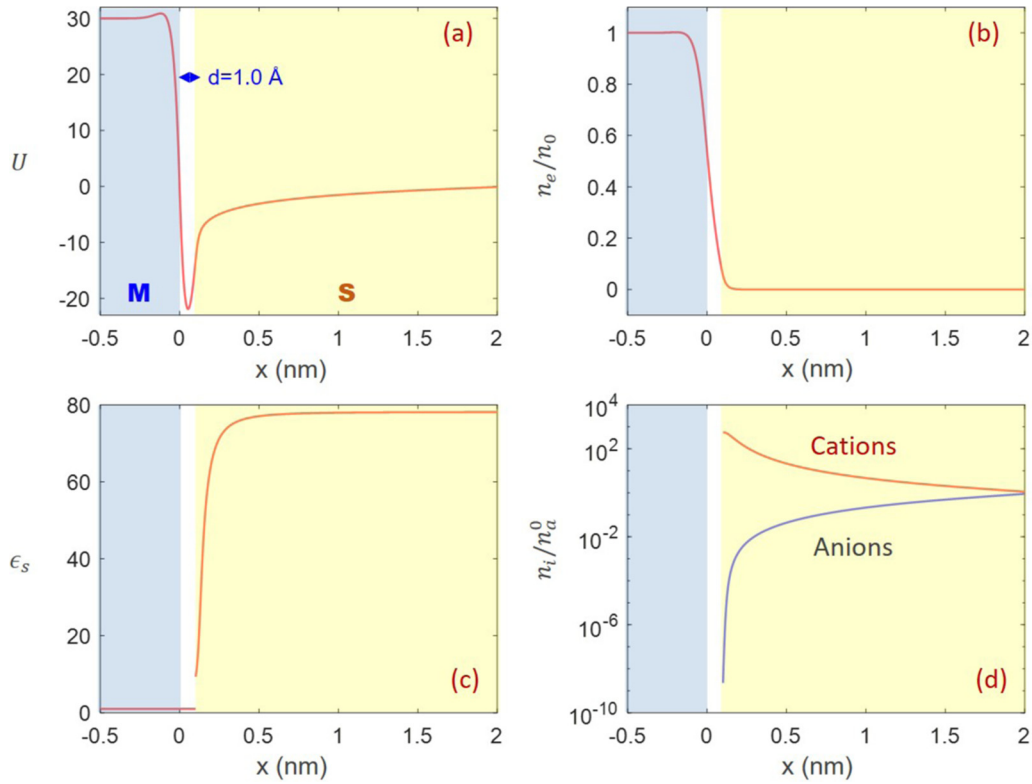


FIG. 2. Model results at $U^{\mathrm{M}} = 30$ (with the potential reference adopted at the solution bulk) for the base case: (a) potential distribution; (b) distribution of free-electron density referenced to its bulk value; (c) distribution of dielectric constant; (d) distributions of cation and anion concentration referenced to its bulk value. The light gray region represents the metal, and the light yellow region represents the solution. The closed plane is located at $d = 1$ Å.

interphase is negatively charged at $U^{\mathrm{M}} = 30$. Figure 2(c) displays the distribution of static dielectric constant $\epsilon_{\mathrm{s}}$. The high electrical field in the interfacial region results in orientation saturation of solvent, namely solvent molecules are reoriented to be more or less parallel with the electric field [43]. Consequently, $\epsilon_{\mathrm{s}}$ decreases to ∼10 at the interface. Figure 2(d) shows that cations are attracted by the negative electrode charge to the interfacial region while anions are repelled.

### B. Calculation of pzc and differential double-layer capacitance

The model is run at a series of electrode potential ranging from 30 to 90 (every 2), with the potential distribution shown in Fig. 3(a). The surface free-charge density of the metal-solution interphase is defined as

$$\sigma^{\mathrm{M}} = \int_{-\infty}^{\infty} (n_0\theta(-x) - n_e) n_{\mathrm{ref}} e_0 dx. \tag{12}$$

Figure 3(b) shows $\sigma^{\mathrm{M}}$ as a function of $U^{\mathrm{M}}$, from which the differential double-layer capacitance, $C_{\mathrm{dl}} = \partial\sigma^{\mathrm{M}}/\partial\phi^{\mathrm{M}}$ ($\phi^{\mathrm{M}}$ is the dimensional counterpart of $U^{\mathrm{M}}$), is obtained and exhibited in Fig. 3(d). $C_{\mathrm{dl}}$ is further divided into an inner-layer part, $C_{\mathrm{inner}} = \partial\sigma^{\mathrm{M}}/\partial(\phi^{\mathrm{M}} - \phi^0)$, with $\phi^0$ being the potential at $x = d$, and an outer-layer part, $C_{\mathrm{outer}} = \partial\sigma^{\mathrm{M}}/\partial(\phi^0)$, correlated through $(C_{\mathrm{dl}})^{-1} = (C_{\mathrm{inner}})^{-1} + (C_{\mathrm{outer}})^{-1}$.

As regards the $\sigma^{\mathrm{M}} \sim U^{\mathrm{M}}$ curve, $\sigma^{\mathrm{M}}$ increases monotonically from negative values at low $U^{\mathrm{M}}$ to positive values at high $U^{\mathrm{M}}$, resulting in a pzc of $U_{\mathrm{pzc}} = 67$ at which $\sigma^{\mathrm{M}} = 0$. More details of the $\sigma^{\mathrm{M}} \sim U^{\mathrm{M}}$ curve are displayed in the $C_{\mathrm{dl}} \sim U^{\mathrm{M}}$ curve in Fig. 3(d). A minimal $C_{\mathrm{dl}}$ is obtained at $U_{\mathrm{minC_{dl}}} = 60$. Deviating from $U_{\mathrm{minC_{dl}}}$ in both directions, $C_{\mathrm{dl}}$ grows due to the increased $C_{\mathrm{outer}}$ and levels off due to the limitation of $C_{\mathrm{inner}}$. A close examination reveals that $C_{\mathrm{dl}}$ is not strictly symmetric around $U_{\mathrm{minC_{dl}}}$. As size symmetry is assumed, this asymmetry has its origin in the metal electronic effect. Specifically, $C_{\mathrm{inner}}$ slightly decreases with increasing $U$, implying that it becomes more difficult to pack electrons into the metal at high potentials.

The deviation between $U_{\mathrm{pzc}}$ and $U_{\mathrm{minC_{dl}}}$ contradicts the conventional notion that these two quantities are equal, throwing doubt on the common practice of obtaining the pzc from the $C_{\mathrm{dl}} \sim U^{\mathrm{M}}$ curve. $U_{\mathrm{minC_{dl}}}$ is, by definition, the potential at which $\sigma^{\mathrm{M}}$ grows slowest as $U^{\mathrm{M}}$ increases. As the whole system is electroneutral, $\sigma^{\mathrm{M}}$ is the negative value of net ionic charge stored in the diffuse layer, which is given by, $\int_d^{\infty}(n_c - n_a)n_{\mathrm{ref}}e_0dx$. At the pzc, $\sigma^{\mathrm{M}} = 0$, we thus have, $\int_d^{\infty}(n_c - n_a)n_{\mathrm{ref}}e_0dx = 0$. However, the total net charge stored in the diffuse layer, given by $\int_d^{\infty}(n_c - n_a - n_e)n_{\mathrm{ref}}e_0dx$, is negative as a portion of metal electrons enter into the diffuse layer. As a result, the potential in the diffuse layer is positive, $U > 0$. Increasing $U^{\mathrm{M}}$ tends to elevate $U$ in the diffuse layer further, and thus shifting $\sigma^{\mathrm{M}}$ to more positive values in an exponential manner, as inferred from Eqs. (8) and (9). This implies that the pzc is more positive than $U_{\mathrm{minC_{dl}}}$ and that $U_{\mathrm{minC_{dl}}}$ should be obtained when $\sigma^{\mathrm{M}} < 0$, namely, at a

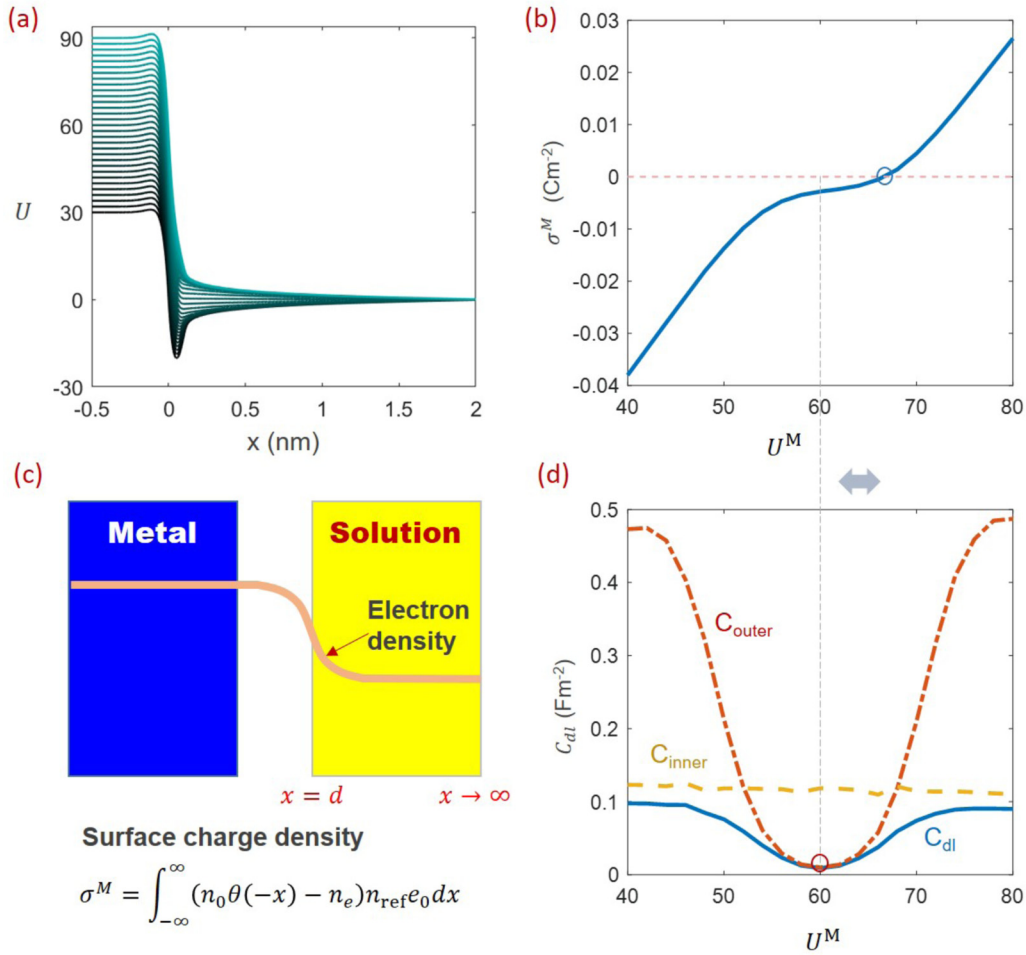


FIG. 3. (a) Potential distribution at a series of electrode potential ranging from 30 to 90 (every 2) for the base case. (b) Surface charging relation of the electrode. (c) The definition of the surface charge density of the metal-solution interphase. The electron density profile is for a schematic illustration. (d) Differential double-layer capacitance, $C_{\rm dl}$, inner-layer capacitance, $C_{\rm inner}$, and outer-layer capacitance, $C_{\rm outer}$, as a function of the electrode potential $U^{\rm M}$.

potential smaller than the pzc, as shown in Figs. 3(b) and 3(d). Interestingly, Uematsu *et al.* recently found that asymmetrical ion adsorption may also lead to the deviation between $U_{\rm pzc}$ and $U_{\rm minC_{dl}}$ [56].

### C. Multifaceted solvent effects

It is well documented that solvent decreases the work function and pzc of metals [2,22,23]. In this vein, two solvent effects have been unraveled in first-principles computational studies [20–23]. On one hand, partial charge transfer from the metal polarizes solvent molecules at the surface, forming surface dipoles. On the other hand, the orthogonalizational repulsion exerted by solvent pushes free electrons back into the metal edge. These two effects are short-range ($\sim r^{-k}, k > 2$) electronic interactions in nature. However, long-range ($\sim r^{-2}$) electrostatic effects of the solvent have not been much discussed before.

Firstly, we examine the effect of $d$ on the pzc in Fig. 4(a). It is found that the pzc shifts to more positive values as $d$ increases. We note that short-range correlations are absent in Fig. 4(a) as we set $W_{\rm s} = 0$ eV. Consequently, the $d$ dependence of the pzc is exclusively caused by long-range electrostatic effects. Specifically, the electrostatic screening effect exerted by the solvent is stronger when $d$ is smaller, decreasing the magnitude of the negative potential outside the metal when $U^{\rm M}$ is lower than the pzc, and thus dragging more electrons out from the metal, namely, $\sigma^{\rm M}$ is more negative, as shown in Fig. 4(a). When $U^{\rm M}$ is higher than the pzc, the magnitude of the positive potential outside the metal decreases, repelling more electrons back into the metal, and resulting in a more positive $\sigma^{\rm M}$. In other words, the $\sigma^{\rm M} \sim U^{\rm M}$ curve gets much steeper as $d$ decreases, namely, $C_{\rm inner}$ and $C_{\rm dl}$ are greater. As depicted in Fig. 4(b), the metal-vacuum interphase is mimicked by placing the solution at a distance large enough, for example, $d > 3$ Å in this model, away from the metal. Consequently, Fig. 4(a) is in line with the usual notion that the pzc of metal-solution interphases ($d$ of several Å) is lower than that calculated from the work function of metal-vacuum interphase (equivalently, $d = \infty$).

Secondly, the solvent changes the fast polarization model of the dielectric medium, reflected in different $\epsilon_{\rm opt}$. The exchange-correlation energy of electrons in Eq. (1) becomes less negative as $\epsilon_{\rm opt}$ increases, pushing free electrons back into the metal edge and decreasing the pzc, as shown in Fig. 4(c). This so-called "polaron effect" was first investigated

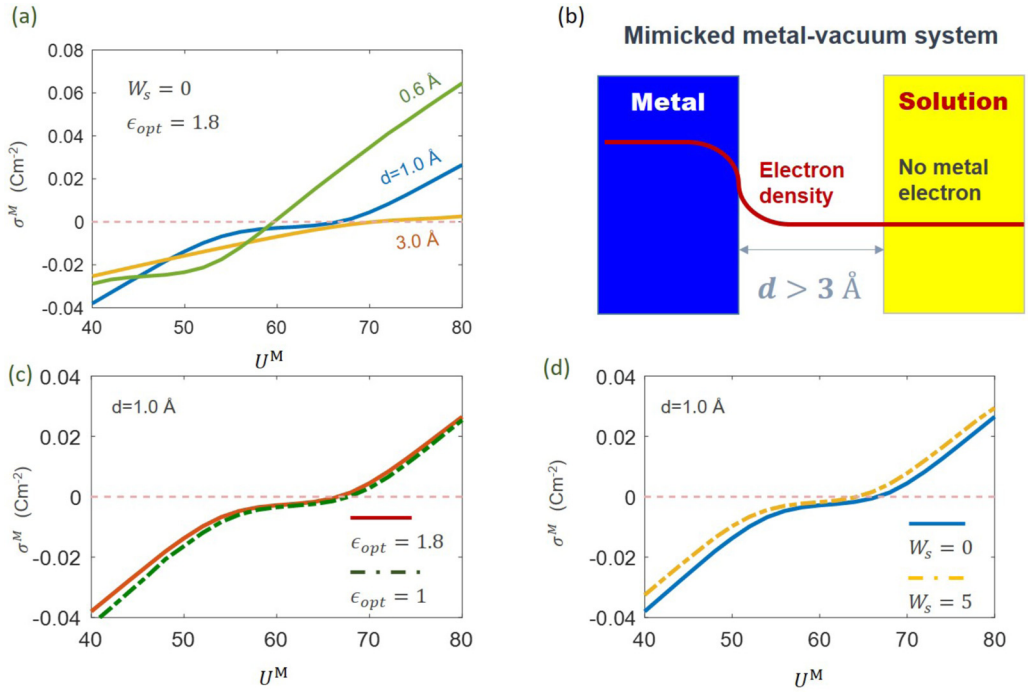


FIG. 4. Solvent effects on the pzc: (a) effect of $d$; (b) mimic of the metal-vacuum interphase ($d > 3$ Å); (c) effect of $\epsilon_{\text{opt}}$, and (d) effect of $W_{\text{s}}$ (unit, eV).

by Kornyshev *et al.*, who used the trial-function approach to solve the jellium model [39,40]. Figure 4(c) shows that the polaron effect on the pzc is only marginal.

Thirdly, another important solvent effect is the orthogonalizational repulsion between solvent and metal electrons, as a consequence of the Pauli repulsion principle [46,47,57]. This orthogonalizational repulsion effect is characterized by a positive $W_{\text{s}}$. Figure 4(d) compares the $\sigma^{\text{M}} \sim U^{\text{M}}$ curve for the cases of $W_{\text{s}} = 0$ and $W_{\text{s}} = 5$ eV. In the presence of orthogonalizational repulsion ($W_{\text{s}} = 5$ eV), electrons are pushed back into the metal edge, resulting in a more positive $\sigma^{\text{M}}$ and thus a lower pzc. As the orthogonalizational repulsion becomes stronger when $d$ is smaller, the decrease in the pzc is greater at smaller $d$.

### D. Specific adsorption of ions

By introducing short-range correlations between ions and solvent into Eq. (1), this model is able to describe specific adsorption of ions and its effect on the surface charging behavior of the metal-solution interphase. As shown in Fig. 5(a), specific adsorption, described by negative $W_{\text{i}}$ $(i = a, c)$ in Eq. (1), shifts $\sigma^{\text{M}}$ to more negative values at potentials far from the pzc, and the pzc changes little though. This is expected as counterions, be they cations or anions, pull free electrons out from the metal, and the concentration of counterions increases dramatically in the interfacial region when the potential deviates from the pzc. For example, at $U^{\text{M}} = 90$, Figs. 5(b) and 5(c) show that anion adsorption results in higher $n_{\text{e}}$ and $n_{\text{a}}$ near the interface ($x = 1$ Å) due to the anion-electron attraction, compared with the case without adsorption. The two curves in Fig. 5(c) intersect as $\sigma^{\text{M}}$ has a lower magnitude for the case with anion adsorption.

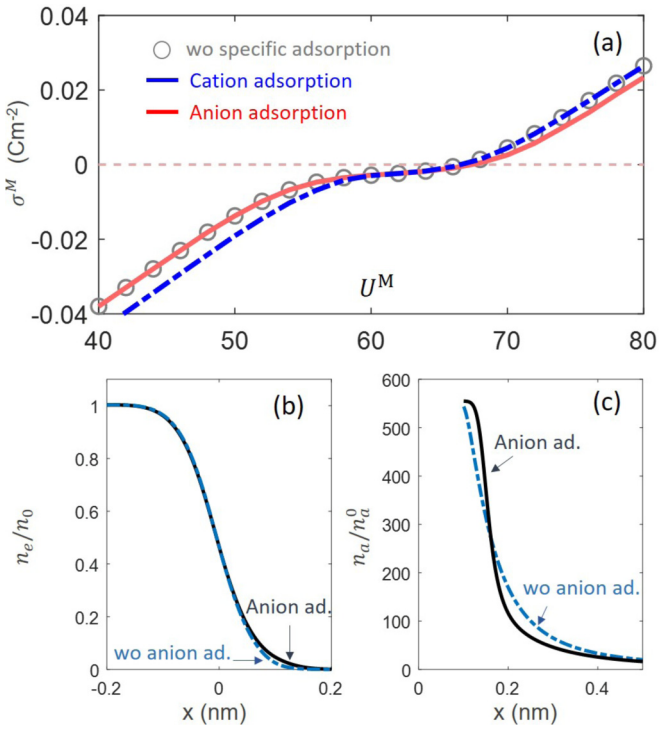


FIG. 5. (a) Effect of specific ionic adsorption on the surface charging curves, $\sigma^{\text{M}} \sim U^{\text{M}}$, for three cases: without specific adsorption ($W_{\text{a}} = W_{\text{c}} = 0$, circles), with cation adsorption ($W_{\text{a}} = 0, W_{\text{c}} = -5$ eV, blue line), and with anion adsorption ($W_{\text{a}} = -5$ eV, $W_{\text{c}} = 0$, red line). (b) and (c) compare free electron ($n_{\text{e}}$) and anion ($n_{\text{a}}$) density profiles at $U^{\text{M}} = 90$, respectively. Herein, we have neglected solvent-electron orthogonalizational repulsion by setting $W_{\text{s}} = 0$.

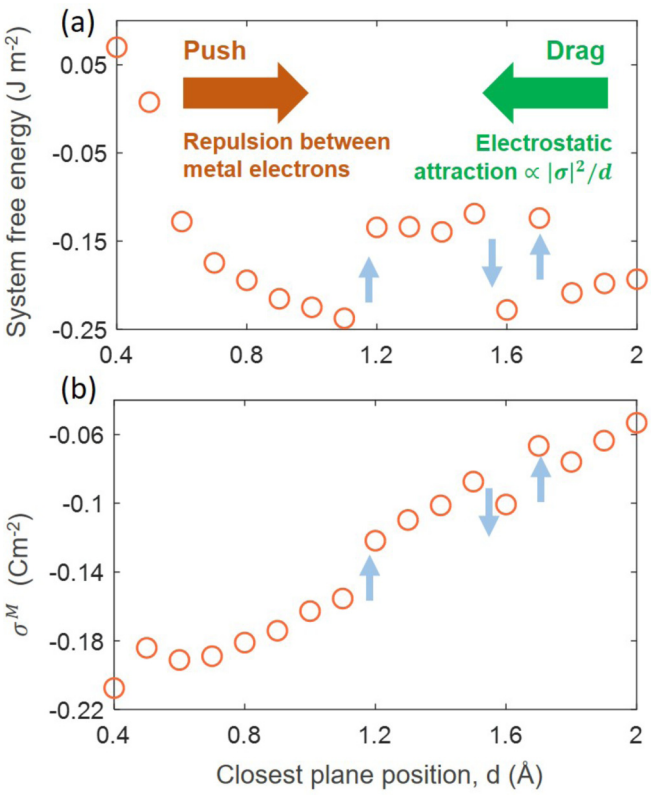


FIG. 6. (a) The system free energy and (b) the metal surface charge density as a function of $d$, the distance of the closest approach of solution species to the electrode. The electrode potential is $U^{\mathrm{M}} = 30$. No short-range correlation is considered, namely, $W_s = W_a = W_c = 0$.

### E. Structure breathing: The end of idyll

From the above analysis, it becomes clear that the structure parameter, $d$, is of primary importance to the pzc, which has been kept constant regardless of the electrode potential in the above discussion. The approximations in this treatment are at least threefold. Firstly, the first solvent layer is hardly coplanar but inevitably corrugated; specifically, the through-plane distance between different water molecules in the first layer can reach 1 Å in the simulation of Sakong and Groß [58]. Secondly, the value of $d$ is usually not static but oscillates all the time. Thirdly, the interfacial structure varies as a function of the electrode potential, termed structure breathing hereinafter. Regarding the third point, Kornyshev *et al.* [59] and Badiali and co-workers [60] developed different approaches to self-consistently determine $d$ for each $\sigma^{\mathrm{M}}$. The essential idea behind the intricate treatment is as follows. The metal and the solution can be roughly regarded as two plates with opposite charge in a capacitor. The attractive electrostatic interactions, together with short-ranged attractive van de Waals forces described in an empirical manner in Ref. [59], in between intend to bring them closer, resulting in a smaller $d$. On the contrary, decreasing $d$ pushes more free electrons back into the metal edge, exacerbating the repulsion between metal electrons. Combined, there exists an optimal $d$ at which the total energy of the metal-solution interphase is minimum.

Figure 6(a) shows how the system free energy (with a constant offset), calculated using Eq. (1), varies as a function of $d$, at $U^{\mathrm{M}} = 30$ for the base case with $W_s = W_a = W_c = 0$ and without introducing more parameters to describe the van de Waals forces. As $d$ increases, the system free energy decreases first due to suppressed repulsion between metal electrons, and then grows, overall speaking, due to attractive electrostatic interactions. Figure 6(b) shows that $\sigma^{\mathrm{M}}$ generally increases with a decreased magnitude as $d$ increases. The erratic changes in $\sigma^{\mathrm{M}}$, marked with arrows, cause nonmonotonic variations in the system free energy. If the system free energy is identical at two $d$ values, the interfacial structure can transition from one to the other, resulting in structural instability similar to that discussed by Partenskii *et al.* [51,53,54]

A key message delivered in Fig. 6 is that $d$ exerts a dramatic influence on the interfacial properties; specifically, $\sigma^{\mathrm{M}}$ varies by $\sim$0.1 $\mathrm{Cm}^{-2}$ when $d$ changes by $\sim$1 Å. Recently, Fernandez-Alvarez and Eikerling developed a hybrid DFT-solvation model for a partially oxidized Pt(111) surface, and also emphasized the importance of $d$. [61] It is an important future step to consider equilibrium values and spatiotemporal statistics of $d$.

## IV. CONCLUDING REMARKS

A jellium-Poisson-Boltzmann model has been developed for metal-solution interphases under constant-potential condition. The model reveals that free metal electrons entering the solution phase cause the deviation between the pzc determined from $\sigma^{\mathrm{M}} \sim U^{\mathrm{M}}$ curves and the potential of Gouy-Chapman minimum extracted from $C_{\mathrm{dl}} \sim U^{\mathrm{M}}$ curves. Multifaceted effects of solvent on the pzc are analyzed, notably that the electrostatic screening effect of solvent leads to a higher pzc when the vacuum gap between the metal surface and the solution phase is larger. The solvent lowers the pzc through two additional effects, viz., the polaron effect and the orthogonalizational repulsion. We further unravel that specific adsorption of ions exerts nontrivial impact on the surface charging behavior, and that $d$, the distance of the closest approach of solution species to the electrode, exerts a dramatic influence on the interfacial properties

Before closing, we reiterate that the pzc is a basic property of the metal-solution interphase, rather than the metal alone. In addition to metal properties that are oft emphasized, solution properties, especially the size, dipole moment, and interfacial arrangement of solvent molecules and specific adsorption of ions, are of equal importance to the pzc. Therefore, the common phrase such as "the pzc of a certain electrode" is not accurate as it does not define the electrolytic solution; given the same metal, the pzc can be dramatically different when it is paired with different electrolytic solutions.

## ACKNOWLEDGMENTS

J.H. acknowledges financial support from National Natural Science Foundation of China (Grant No. 21802170), and Central South University (Grant No. 502045001). S.C. acknowledges financial support from Natural Science Foundation of China (Grant No. 21832004). J.H. is indebted to Prof. Kornyshev for stimulating discussion.

[1] A.J. Bard, G. Inzelt, and F. Scholz, *Electrochemical Dictionary* (Springer-Verlag, Berlin, 2008).

[2] S. Trasatti and E. Lust, in *Modern Aspects of Electrochemistry*, edited by R. E. White, J. O. M. Bockris, and B. E. Conway (Springer, Boston, 1999).

[3] J. Huang, J. Zhang, and M. Eikerling, Phys. Chem. Chem. Phys. **20**, 11776 (2018).

[4] R. Rizo, E. Sitta, E. Herrero, V. Climent, and J. M. Feliu, Electrochim. Acta **162**, 138 (2015).

[5] J. Huang and S. Chen, J. Phys. Chem. C **122**, 26910 (2018).

[6] C. Lin, E. Laborda, C. Batchelor-McAuley, and R. G. Compton, Phys Chem. Chem. Phys. **18**, 9829 (2016).

[7] A. Frumkin and A. Gorodetzkaja, Z. Phys. Chem. **136**, 451 (1928).

[8] A. Frumkin, O. Petry, and B. Damaskin, J. Electroanal. Chem. **27**, 81 (1970).

[9] A. N. Frumkin and O. A. Petrii, Electrochim. Acta **20**, 347 (1975).

[10] A. N. Frumkin, O. A. Petrii, and B. B. Damaskin, in *Comprehensive Treatise of Electrochemistry*, edited by J. O. M. Bockris, B. E. Conway, and E. Yeager (Springer, Boston, 1980).

[11] O. A. Petrii, Russian J. Electrochem. **49**, 401 (2013).

[12] V. Briega-Martos, E. Herrero, and J. M. Feliu, Curr. Opin. Electrochem. **17**, 97 (2019).

[13] V. Climent and J. M. Feliu, J. Solid State Electrochem. **15**, 1297 (2011).

[14] V. Climent, G. A. Attard, and J. M. Feliu, J. Electroanal. Chem. **532**, 67 (2002).

[15] T. Pajkossy, T. Wandlowski, and D. M. Kolb, J. Electroanal. Chem. **414**, 209 (1996).

[16] A. Cuesta, Surf. Sci. **572**, 11 (2004).

[17] N. Garcia-Araez, V. Climent, and J. Feliu, J. Phys. Chem. C **113**, 9290 (2009).

[18] R. Martínez-Hincapié, V. Climent, and J. M. Feliu, Electrochem. Commun. **88**, 43 (2018).

[19] R. Martínez-Hincapié, V. Climent, and J. M. Feliu, Curr. Opin. Electrochem. **14**, 16 (2019).

[20] R. Jinnouchi and A. B. Anderson, Phys. Rev. B **77**, 245417 (2008).

[21] V. Tripkovic, M. E. Björketun, E. Skúlason, and J. Rossmeisl, Phys. Rev. B **84**, 115452 (2011).

[22] S. Sakong, K. Forster-Tonigold, and A. Groß, J. Chem. Phys. **144**, 194701 (2016).

[23] J. Le, M. Iannuzzi, A. Cuesta, and J. Cheng, Phys. Rev. Lett. **119**, 016801 (2017).

[24] J. Cheng and M. Sprik, Phys. Chem. Chem. Phys. **14**, 11245 (2012).

[25] M. J. Eslamibidgoli and M. H. Eikerling, Curr. Opin. Electrochem. **9**, 189 (2018).

[26] O. M. Magnussen and A. Groß, J. Am. Chem. Soc. **141**, 4777 (2019).

[27] K. Letchworth-Weaver and T. A. Arias, Phys. Rev. B **86**, 075140 (2012).

[28] M. M. Melander, M. J. Kuisma, T. E. K. Christensen, and K. Honkala, J. Chem. Phys. **150**, 041706 (2018).

[29] J. Huang, A. Malek, J. Zhang, and M. H. Eikerling, J. Phys. Chem. C **120**, 13587 (2016).

[30] J. Huang, T. Zhou, J. Zhang, and M. Eikerling, J. Chem. Phys. **148**, 044704 (2018).

[31] P. Hohenberg and W. Kohn, Phys. Rev. **136**, B864 (1964).

[32] W. Kohn and L. J. Sham, Phys. Rev. **140**, A1133 (1965).

[33] N. D. Lang and W. Kohn, Phys. Rev. B **1**, 4555 (1970).

[34] N. D. Lang, in *Solid State Physics*, edited by H. Ehrenreich, F. Seitz, and D. Turnbull (Academic, New York, 1974).

[35] J. P. Badiali, M. L. Rosinberg, F. Vericat, and L. Blum, J. Electroanal. Chem. **158**, 253 (1983).

[36] J. P. Badiali, M. L. Rosinberg, and J. Goodisman, J. Electroanal. Chem. **130**, 31 (1981).

[37] W. Schmickler, J. Electroanal. Chem. **150**, 19 (1983).

[38] J. R. Smith, Phys. Rev. **181**, 522 (1969).

[39] A. A. Kornyshev, A. M. Kuznetsov, G. Makov, and M. V. Vigdorovitch, J. Chem. Soc., Faraday Trans. **92**, 3997 (1996).

[40] A. A. Kornyshev, A. M. Kuznetsov, G. Makov, and M. V. Vigdorovitch, J. Chem. Soc., Faraday Trans. **92**, 4005 (1996).

[41] J. D. Jackson, *Classical Electrodynamics* (Wiley, New York, 1999).

[42] F. Booth, J. Chem. Phys. **19**, 391 (1951).

[43] E. Gongadze and A. Iglič, Bioelectrochem. **87**, 199 (2012).

[44] A. A. Kornyshev, J. Phys Chem. B **111**, 5545 (2007).

[45] Y. Zhang and J. Huang, J. Phys. Chem. C **122**, 28652 (2018).

[46] W. Schmickler and D. Henderson, J. Chem. Phys. **80**, 3381 (1984).

[47] W. Schmickler and D. Henderson, J. Chem. Phys. **85**, 1650 (1986).

[48] A. A. Kornyshev, Electrochim. Acta **34**, 1829 (1989).

[49] W. Schmickler, Chem. Rev. **96**, 3177 (1996).

[50] M. B. Partenskii, V. Dorman, and P. C. Jordan, Int. Rev. Phys. Chem. **15**, 153 (1996).

[51] M. B. Partenskii and P. C. Jordan, Phys. Rev. E **80**, 011112 (2009).

[52] V. J. Feldman, M. B. Partenskii, and M. M. Vorob'ev, Prog. Surf. Sci. **23**, 3 (1986).

[53] M. B. Partenskii and P. C. Jordan, J. Chem. Phys. **99**, 2992 (1993).

[54] M. B. Partenskii and P. C. Jordan, Am. J. Phys. **79**, 103 (2010).

[55] A. Y. Lozovoi, A. Alavi, J. Kohanoff, and R. M. Lynden-Bell, J. Chem. Phys. **115**, 1661 (2001).

[56] Y. Uematsu, R. R. Netz, and D. J. Bonthuis, J. Phys.: Condens. Matter **30**, 064002 (2018).

[57] Z. B. Kim, A. A. Kornyshev, and M. B. Partenskii, J. Electroanal. Chem. **265**, 1 (1989).

[58] S. Sakong and A. Groß, J. Chem. Phys. **149**, 084705 (2018).

[59] V. I. Feldman, A. A. Kornyshev, and M. B. Partenskii, Solid State Commun. **53**, 157 (1985).

[60] S. Amokrane, V. Russier, and J. P. Badiali, Surf. Sci. **210**, 251 (1989).

[61] V. M. Fernandez-Alvarez and M. H. Eikerling, ACS Appl. Mater. Interfaces. **11**, 43774 (2019).